

Journal Pre-proof

A facile method for classifying starch fractions rich in long linear dextrin

Chengdeng Chi, Youcai Zhou, Bilian Chen, Yongjin He, Yingting Zhao

PII: S0268-005X(22)00702-0

DOI: <https://doi.org/10.1016/j.foodhyd.2022.108182>

Reference: FOOHYD 108182

To appear in: *Food Hydrocolloids*

Received Date: 31 August 2022

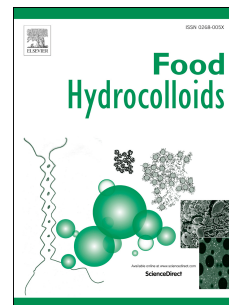
Revised Date: 17 September 2022

Accepted Date: 21 September 2022

Please cite this article as: Chi, C., Zhou, Y., Chen, B., He, Y., Zhao, Y., A facile method for classifying starch fractions rich in long linear dextrin, *Food Hydrocolloids* (2022), doi: <https://doi.org/10.1016/j.foodhyd.2022.108182>.

This is a PDF file of an article that has undergone enhancements after acceptance, such as the addition of a cover page and metadata, and formatting for readability, but it is not yet the definitive version of record. This version will undergo additional copyediting, typesetting and review before it is published in its final form, but we are providing this version to give early visibility of the article. Please note that, during the production process, errors may be discovered which could affect the content, and all legal disclaimers that apply to the journal pertain.

© 2022 Published by Elsevier Ltd.



A facile method for classifying starch fractions rich in long linear dextrin

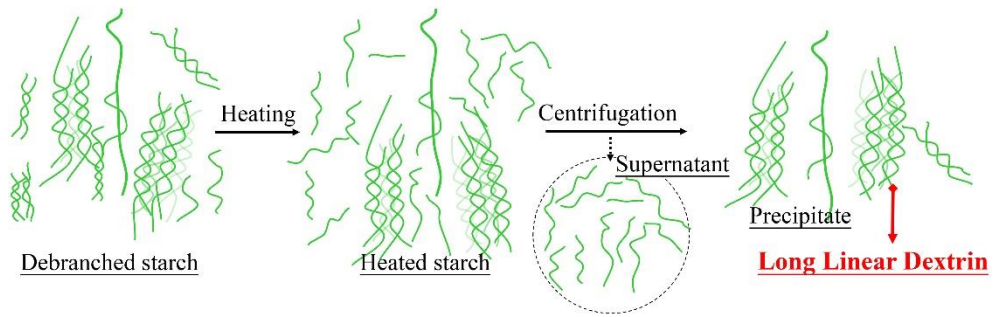
Chengdeng Chi ^{a,*}, Youcai Zhou ^a, Bilian Chen ^a, Yongjin He ^a, Yingting Zhao ^{b,*}

^a College of Life Sciences, Fujian Normal University, Fuzhou 350117, China

^b The University of Queensland, Queensland Alliance for Agriculture and Food Innovation, Brisbane, QLD, 4072, Australia

*Corresponding author: Chengdeng Chi and Yingting Zhao

Email address: c_cd@fjnu.edu.cn (C. Chi) and yingting.zhao@uqconnect.edu.au (Y. Zhao)



Journal Pre-proof

1 **Abstract**

2 Fractionation of linear dextrans with different chain lengths was of great
3 significance for the preparation of functional foods. Traditional gradient non-solvent
4 precipitation method for the fractionation was time-consuming and labor-intensive,
5 making it inconvenient for large-scale dextrin fractionation. The aim of this study was
6 to establish a novel method to fractionate long linear dextrans from debranched waxy
7 maize starch by simply heating (70-80 °C) and centrifuging the debranched starch
8 solution. The results showed that the linear dextrans produced during the debranching
9 process formed ordered structures with melting temperature of 58.8-95.4 °C. According
10 to the analysis of starch thermostability and chain length distribution, it was found that
11 thermostability of ordered structure was significantly and positively correlated with the
12 chain length of linear dextrans. During heating at 70 and 80 °C, less ordered structures
13 with weak thermostability were melted in solution, herein short linear dextrans were
14 removed from debranched starch via centrifugation and thermostable ordered structures
15 could be fractionated to obtain long linear dextrans. By this simple “heating-
16 centrifugation” method, the content of long linear dextrans in starches was increased
17 from 27.08% to 43.40%. This study provided a promising pathway to fractionate long
18 linear dextrans.

19

20 **Keywords**

21 Starch fractionation, linear dextrans, chain length distribution, molecular size, starch
22 thermostability

23 1. Introduction

24 Starch consisted of two groups of glucose polymers: (i) amylose, which was a
25 linear polysaccharide made of α -D-glucose units, and (ii) amylopectin, which was a
26 highly branched polymer of α -D-glucose units. Linear dextrin was a type of linear
27 glucan derived from amylopectin following debranching enzymes such as isoamylase
28 and pullulanase (Liu et al., 2017). It had great applications in many fields such as foods,
29 pharmaceuticals, and functional materials (Liu et al., 2017), *e.g.*, it readily formed gel
30 networks and crystalline structures to slow starch enzymatic digestion (Liu et al., 2017),
31 or formed nanoparticles to stabilize emulsion (Ge et al., 2017), or interacted with other
32 ingredients, such as ethylene and curcumin, to form intelligent carriers to protect these
33 bioactive factors from degradation or rapid escape (Liu et al., 2022; Sun, Tian, Chen,
34 & Jin, 2017). Notably, increasing the length of linear dextrin promoted starch
35 reassembly to slow starch digestion (Chang et al., 2019), and enabled non-starchy
36 ingredients such as ethylene and curcumin to interact with the dextrin, resulting in an
37 ideal delivery system with controllable release behaviors (Liu et al., 2022; Sun et al.,
38 2017; Zhan et al., 2021). Accordingly, fractionation of long-chain linear dextrans was
39 rather important to control functionalities of foods prepared from the linear dextrans.

40 Fractionation of polysaccharides was mostly performed by chromatography,
41 ultrafiltration and gradient non-solvent precipitation (Hu & Goff, 2018).
42 Chromatography and ultrafiltration required columns and membranes, which limited
43 their applications in polysaccharide fractionation because of their high equipment
44 investment and operating costs (Hu et al., 2018). Fractionation by gradient non-solvent

45 precipitation corresponded to the gradual addition of a non-solvent (*e.g.*, methanol,
46 ethanol, isopropanol, acetone and 1-butanol) into the polysaccharide solution to
47 gradually precipitate the polysaccharides the solution. Long linear dextrin had a lower
48 solubility in non-solvent solution compared with short linear dextrin, and herein long
49 linear dextrin could be obtained via controlling the non-solvent content in the solution
50 (Hu et al., 2018). As the gradient non-solvent precipitation was independent of special
51 equipment and required simple equipment such as stirred tanks and centrifuges, it was
52 herein widely used in dextrin fractionation (Chang et al., 2018; Hu et al., 2018; Qiu et
53 al., 2016). However, the operation for the gradient non-solvent precipitation was time-
54 consuming and labor-intensive, making this method inconvenient for large-scale
55 dextrin fractionation. The development of a facile and feasible fractionation method
56 will be helpful to isolate long linear dextrans with high efficiency.

57 It was noted that amylopectin with longer chain length tended to show a higher
58 thermostability in solution (Wang et al., 2021; Zhang, Wang, Chen, & Zhong, 2019;
59 Zhang et al., 2017), indicating ordered structures packed with long amylopectin may
60 endure hot solution while less ordered structures formed with short amylopectin
61 probably dissolved in solution during the heating. Accordingly, we hypothesized that
62 helical structures packed with long linear dextrans had high thermostability and
63 therefore likely to tolerate heated solutions. If helical and crystalline structures formed
64 by linear dextrans were heated with controllable temperature in solution, the structures
65 packed with short linear dextrans were expected to dissolve in solution, and then ordered
66 structures formed by long linear dextrans could be obtained from the solution via

67 centrifugation (**Figure 1**). Results will offer a promising pathway to fractionate long
68 linear dextrin-rich starch.

69 **2. Materials and methods**

70 **2.1 Materials**

71 Waxy maize starch (WMS) was purchased from Suzhou Gaofeng Starch
72 Technologies Co., Ltd. (Suzhou, China). The contents of amylose, protein, lipid, and
73 moisture of WMS were 0.20%, 0.02%, 0.01%, and 10.52%, respectively. Pullulanase
74 (EC 3.2.1.41, enzyme activity 1000 U/mL) was purchased from Novozymes (batch No.
75 ATS20059; Tianjin, China). Isoamylase (EC 3.2.1.68, enzyme activity ≥ 10000000
76 units/mg protein) and acetate was purchased from Sigma. Sodium azide solution was
77 purchased from Sangon Biotech Co., Ltd (Shanghai, China). Ultra-pure water was
78 prepared using a Milli-Q water purification system (Millipore, Bedford, MA, USA).
79 Other reagents used were analytical grade.

80 **2.2 Preparation of debranched starch**

81 Starch suspension with a concentration of 10% (w/v) was prepared and cooked at
82 100 °C for 30 min. The temperature of cooked starch was cooled to 58 °C and the pH
83 was adjusted to 5.2. Gelatinized starch was then fully debranched by pullulanase at 240
84 ASPU/g starch for 24 h (Shi, Sweedman, & Shi, 2018). Afterwards, starch suspension
85 was frozen at -80 °C for 6 h and freeze-dried using a lyophilizer. The dried starches
86 were added with ethanol to denature the pullulanase and dried at 40 °C for 24 h. Finally,
87 samples were ground and sieved for further analysis. Debranched waxy maize starch
88 was abbreviated as DWMS.

89 **2.3 Classification of linear dextrin from debranched starch**

90 Debranched starch was added with distilled water at 25 °C until the concentration
91 was 5% (w/v). The suspension was heated at 60-90 °C for 20 min and its visual
92 appearance was recorded using a camera. Additionally, the suspensions heated at 70
93 and 80 °C were centrifuged (5000 r/min, 5 min) immediately after the heating. The
94 precipitate and supernatant were cooled to 25 °C and frozen at -80 °C for 6 h and freeze-
95 dried using a lyophilizer. The precipitates isolated from heated DMS were abbreviated
96 as P70 and P80, respectively, and the corresponding supernatants were abbreviated as
97 S70 and S80, respectively.

98 **2.4 Gelatinization properties of starches**

99 Starch in a high-pressure stainless pan was added with distilled water to prepare
100 starch suspension with a concentration of 30% (w/w). The pan was sealed with a gold-
101 plated copper and equilibrated at 25 °C for 12 h before DSC analysis. An empty pan
102 was used as a reference. Sample was heated from 30 to 130 °C at a scanning rate of
103 10 °C/min. The onset temperature (T_o) and end temperature (T_e) were calculated using
104 DSC software (TA Instruments, New Castle, DE, USA) to evaluate starch
105 thermostability.

106 In particular, S80 after the heating was cooled from 130 to 30 °C at a cooling rate
107 of 10 °C/min, and then immediately heated from 30 to 130 °C at a scanning rate of
108 10 °C/min, to unravel how linear dextrin reassembled during the cooling. Rescanned
109 S80 was abbreviated as S80-rescan-X, while the “X” corresponded to rescanning times.

110 **2.5 Fine structures of starches**

111 Molecular weight distributions of starches were characterized by a previous
112 method (Zhao, Henry, & Gilbert, 2021) with slight modifications. Sample (5 mg) was
113 thoroughly mixed with 5 mL of DMSO solution containing lithium bromide (0.5% w/w)
114 (DMSO/LiBr) and heating at 90 °C using a thermomixer for 3 h. The molecular weight
115 of starch sample was analyzed using size exclusion chromatography equipped with a
116 differential refractive index detector (Optilab T-rEX, Wyatt Technology Co., Santa
117 Barbara, CA, USA) (SEC-RI), two tandem columns (300 × 8 mm, Shodex OH-pak SB-
118 805 and 803; Showa Denko K.K., Tokyo, Japan) which was held at 60 °C using a model
119 column heater. The flow rate of mobile phase (DMSO/LiBr) was 0.3 mL/min. Standard
120 dextrans of known molecular weights (342, 3650, 21000, 131400, 610500, 821700,
121 3755000) were used for column calibration. Data were acquired and processed using
122 ASTRA6.1 (Wyatt Technology).

123 Additionally, starches were further treated with isoamylase and then detected with
124 high-performance anion-exchange chromatography (HPAEC) on a CarboPac PA-200
125 anion-exchange column (4.0 × 250 mm; Dionex) using a pulsed amperometric detector
126 (PAD; Dionex ICS 5000 system). Starch (10 mg) was dissolved in 5 mL of water in a
127 boiling water bath for 60 min. Sodium azide solution (5 µL, 40 mg/mL), acetate buffer
128 (0.1 mL, 0.1 M, pH 3.5), and isoamylase (2.5 µL) were added to starch solution, and
129 the mixture was incubated in a water bath at 37 °C for 24 h. The hydroxyl groups of the
130 debranched glucans were reduced by treatment with sodium borohydride (0.5%, w/v)
131 under alkaline conditions for 20 h. Then, about 600 µL solution was dried in vacuo at

132 room temperature and redissolved in 30 μL of NaOH solution (1 M) for 60 min. The
133 solution was diluted with 570 μL of distilled water and determined on ICS 5000 system
134 with flow rate of mobile phase of 0.4 mL/min, injection volume of 5 μL , and mobile
135 phase of NaOH solution (0.2 M NaOH, 0.2 M NaAc) with a gradient program: 90:10
136 (v/v) at 0 min, 90:10 (v/v) at 10 min, 40:60 (v/v) at 30 min, 40:60 (v/v) at 50min, 90:10
137 (v/v) at 50.1 min, and 90:10 (v/v) at 60 min. Data acquired on the ICS5000 (Thermo
138 Scientific) were processed using chromeleon 7.2 CDS (Thermo Scientific). Technical
139 support is provided by Sanshu Biotech. Co., LTD (Shanghai, China).

140 **2.6 Statistical analysis**

141 All tests were conducted at least in triple and the data were analyzed using IBM
142 SPSS statistics version 21.0 (IBM, Armonk, NY, USA) by means of analysis of variance
143 (ANOVA), followed by the Turkey's HSD test to compare the treatments and the
144 significance level was set at $P < 0.05$.

145 **3. Results and discussion**

146 **3.1 Visual appearance of debranched starch solutions at different** 147 **temperatures**

148 **Figure 2** showed the visual appearance of debranched starch solutions at different
149 temperatures. The debranched starch solution was milky and untransparent at 25 $^{\circ}\text{C}$,
150 because starch particles with ordered structures did not dissolve in cold solution. The
151 solution gradually became transparent as the temperature increased from 60 to 90 $^{\circ}\text{C}$.
152 Notably, the heated solutions at 70 and 80 $^{\circ}\text{C}$ also contained starch particles in solution,
153 indicating the heated solutions contained some thermostable starch structures. If starch

154 thermostability was highly correlated with starch chain length, starch structures packed
155 with long linear dextrans could be fractionated via heating the starch solution and
156 dissolving the less ordered structures in solution at 70 and 80 °C. Herein, solutions
157 heated at 70 and 80 °C were centrifuged to obtain the supernatants and precipitates to
158 verify whether long linear dextrans contributed to the formation of thermostable starch
159 particles and whether long linear dextrans could be obtained by the proposed method as
160 shown in **Figure 1**.

161 **3.2 Thermal properties of starches**

162 Thermal properties of starches were shown in **Figure 3** and **Table 1**. Both WMS
163 and DWMS exhibited a phase transition peak (G) over DSC curves, corresponding to
164 the melting of helical structures (Liu et al., 2009). Cooked WMS generally did not
165 contain ordered structures but DWMS contained a relatively high content of helical
166 structures. Ordered structures of DWMS must be attributed to the reassembly of linear
167 dextrans during the pullulanase treatment. Notably, the gelatinization of DWMS started
168 at 58.8 °C and ended at 95.4 °C, confirming that the debranched starch partially melted
169 in solution as the temperature increased from 60 °C to 90 °C.

170 Fractionated starches also showed a peak over DSC curves, indicating that all the
171 starches contained relatively high content of helical structures. P70 and P80 gelatinized
172 at 87.9-116.2 °C and 94.0-120.2 °C, respectively, suggesting that the prepared starches
173 had thermostable structures. P80 exhibited a higher gelatinization temperature than P70,
174 confirming that more less ordered structures were removed from DWMS for preparing
175 P80. Additionally, the gelatinization temperatures of P70 and P80 were higher than 70

176 and 80 °C, respectively, which were mostly attributed to the reassembly of starch
177 structures during heating treatment in terms of annealing (Chi et al., 2019). As S70 and
178 S80 were prepared from the supernatant of the solution, S70 and S80 could probably
179 not contain ordered structures because the supernatant only contained some linear
180 dextrans and amorphous structures. However, linear dextrans would form helical and
181 crystalline structures in 30 min at 4 °C (Sun, Gong, Li, & Xiong, 2014). This study also
182 found that S80 after gelatinization and cooling still showed a peak over DSC curve
183 during rescanning (**Figure S1** and **Table S1**), confirming that gelatinized S80 would
184 form helical structures rapidly.

185 **3.3 Starch molecular weight distributions**

186 The molecular size distribution of WMS and debranched starches was analyzed
187 using SEC-RI chromatograms. The RI response (**Figure 4A**) and relationships between
188 SEC weight distributions ($w(\log(V_h))$) and molecular size (R_h) of starches (**Figure 4B**)
189 were obtained. According to **Figure 4A**, one elution peak was observed at 35-60 min
190 for WMS, corresponding to the elution of amylopectin. After pullulanase treatment, the
191 peak shifted towards higher elution time, confirming hydrolytic degradation and a
192 decrease in molar mass (Vidal, Bai, Geng, & Martinez, 2022). Notably, DWMS showed
193 three elution peaks at *ca.* 50-65 min, 71-77 min, and 77-90 min, which were probably
194 assigned to amylopectin with low molar mass, long linear dextrans, and linear dextrans,
195 respectively. S70 and S80 only contained an elution peak at 65-90 min, suggesting S70
196 and S80 mostly contained only linear dextrans. Whilst, P70 and P80 showed three peaks
197 at *ca.* 50-65 min, 71-77 min, and 77-90 min, confirming these two starches contained

198 small amylopectin, long linear dextrans, and short linear dextrans. Comparing with
199 DWMS, P70 and P80, especially the P80, had higher peak intensity at 50-65 min and
200 71-77 min, suggesting these starches contained more small amylopectin and long linear
201 dextrans.

202 According to **Figure 4B**, the molecular size (R_h) of WMS was *ca.* 30-200 nm,
203 while the R_h of all debranched starch was much smaller (< 40 nm), confirming the
204 degradation of starch during the pullulanase treatment (Li et al., 2020). Zhao et al. (2021)
205 reported that starch chains with a R_h of *ca.* 30 nm were the amylopectin with low molar
206 mass. Starch possibly produced small amylopectin with low molar mass during the
207 debranching, and herein the fraction with R_h of 5-80 nm mostly assigned to small
208 amylopectin. That further confirmed that DWMS, P70, and P80 contained some small
209 amylopectin. Notably, P70 and P80, especially the P80, showed higher peak intensity
210 at the range of $1.7 < R_h < 5.0$ nm, suggesting these two starches contained more long
211 linear dextrans.

212 Molecular weight distribution of starch was also shown in **Table 2**. All fractions
213 of WMS showed molar mass higher than 800k g/mol. After pullulanase treatment,
214 starches did not contain fraction larger than 800k g/mol, confirming starch degradation.
215 Comparing with DWMS, S70 and S80 did not contain the fractions of $80k < M_w < 800k$
216 g/mol (DP 500-5000) but contained less fractions of $8k < M_w < 80k$ g/mol (DP 50-500)
217 and more fractions of $M_w < 8k$ g/mol (DP < 50), suggesting S70 and S80 mostly
218 contained more short linear dextrans. P70 and P80 contained more fractions of $80k <$
219 $M_w < 800k$ g/mol comparing with DWMS, S70, and S80, corresponding to higher

220 content of small amylopectin. Additionally, P70 and P80, especially the P80, showed a
221 lower proportion of fraction of $M_w < 5k$ g/mol but higher proportions of fractions of $5k$
222 $< M_w < 8k$ g/mol (DP 31-50) and $8k < M_w < 80k$ g/mol (DP 50-500), indicating these
223 two starches probably contained more long linear dextrans.

224 **3.4 Chain length distribution of starches**

225 High-performance anion-exchange chromatograms of debranched starches were
226 shown in **Figure S2**, and the chain length distribution of amylopectin were summarized
227 in **Table 3**. The average chain length of different starches showed in the orders of S70
228 $< S80 < DWMS < P70 = P80$, indicating our proposed fractionation method showed
229 high efficiency in fractionating long chain length. Comparing with DWMS, S70 and
230 S80 showed more fractions of DP 6-24. S80 contained more fractions of DP > 25 in
231 comparison with S70. Ordered structures packed with longer amylopectin showed
232 higher thermostability (Wang et al., 2021; Zhang et al., 2019; Zhang et al., 2017).
233 Accordingly, the supernatant of heated debranched starch solution contained more long
234 chains at 80 °C than that at 70 °C. P70 and P80 displayed less fractions of DP 6-24 and
235 more fractions of DP > 25 comparing with DWMS. Additionally, P80 contained more
236 fractions of DP ≥ 37 than P70 did, suggesting the heating at 80 °C favored the
237 fractionation of long chains. According to **Figure 4**, P70 and P80 showed high peak
238 intensity at the range of $1.7 < R_h < 5.0$ nm (long linear dextrans). Herein, the long chains
239 of P70 and P80 were assigned to long linear dextrans rather amylopectin with long chain
240 length. That confirmed that our proposed method could be used for isolating long linear
241 dextrans from debranched waxy maize starch via simply heating the solution containing

242 debranched starch.

243 **3.5 Underlying mechanism for the fraction of long linear dextrans**

244 Structural changes of starch structures during the fraction of long linear dextrans
245 were shown in **Figure 5**. Debranched starch produced during the pullulanase treatment
246 formed ordered structures with melting temperature of 58.8-95.4 °C (**Table 1**).
247 Thermostability of ordered structure was positively correlated with chain length of
248 linear dextrans (**Table 1** and **Table 3**). Accordingly, debranched starch partially
249 gelatinized and contributed to the melting of less ordered structures in solution at 70
250 and 80 °C, and then released the short linear dextrans (**Table 2** and **Table 3**). The
251 supernatant of the centrifuged solution herein contained a relatively high content of
252 short linear dextrans. Notably, the short linear dextrans probably with DP 13-24 (**Table**
253 **3**) formed helical and crystalline structures rapidly during the cooling. Accordingly, the
254 short linear dextrans separated from the supernatant could be used to prepare functional
255 starch rich in helical and crystalline structures. On the other hand, the precipitates were
256 rich in long linear dextrans because of the removal of short linear dextrans. It seemed
257 that the thermostability of ordered structures determined the fractionation of long linear
258 dextrin according to our proposed “heating-centrifugation” method. Ordered structures
259 packed with long linear dextrans could tolerate hydrothermal treatment, and in turn,
260 thermostable ordered structures could be obtained via removing the short linear dextrans
261 simply by “heating-centrifugation” method to obtain starch rich in long linear dextrans.

262 **Conclusions**

263 In this study, we opened a promising pathway to fractionate long linear dextrin-

264 rich starch from DWMS by simply heating and centrifuging the debranched starch
265 solution. Linear dextrans produced during the debranching process formed ordered
266 structures with melting temperature of 58.8-95.4 °C. Whilst, thermostability of ordered
267 structures was significantly and positively correlated with chain length of linear
268 dextrans. During heating at 70 or 80 °C, less ordered structures with weak
269 thermostability were melted in solution and herein the short linear dextrans could be
270 removed by centrifuging the solution to obtain long linear dextrin-rich starch. It seemed
271 that the heating at high temperature (below the end temperature of starch gelatinization)
272 will be helpful to fractionate long linear dextrans. Although this study verified the
273 “heating-centrifugation” method could be used for fractionating long linear dextrin-rich
274 starch, how temperature and centrifugal force affected the fractionation efficiency of
275 long linear dextrans should be further investigated in the future. Additionally,
276 physicochemical properties and functionalities of these fractionated starch were also
277 parts of our future works.

278 **Funding**

279 The research was financially supported from the Scientific Research Innovation
280 Program “Xiyuanjiang River Scholarship” of College of Life Sciences, Fujian Normal
281 University.

282 **References**

283 Chang, R., Li, M., Wang, Y., Chen, H., Xiao, J., Xiong, L., Qiu, L., Bian, X., Sun, C.,
284 & Sun, Q. (2019). Retrogradation behavior of debranched starch with different
285 degrees of polymerization. *Food Chemistry*, 297, 125001.

- 286 Chang, R., Xiong, L., Li, M., Liu, J., Wang, Y., Chen, H., & Sun, Q. (2018).
287 Fractionation of debranched starch with different molecular weights via edible
288 alcohol precipitation. *Food Hydrocolloids*, 83, 430-437.
- 289 Chi, C., Li, X., Lu, P., Miao, S., Zhang, Y., & Chen, L. (2019). Dry heating and
290 annealing treatment synergistically modulate starch structure and digestibility.
291 *International Journal of Biological Macromolecules*, 137, 554-561.
- 292 Ge, S., Xiong, L., Li, M., Liu, J., Yang, J., Chang, R., Liang, C., & Sun, Q. (2017).
293 Characterizations of Pickering emulsions stabilized by starch nanoparticles:
294 Influence of starch variety and particle size. *Food Chemistry*, 234, 339-347.
- 295 Hu, X., & Goff, H. D. (2018). Fractionation of polysaccharides by gradient non-solvent
296 precipitation: A review. *Trends in Food Science & Technology*, 81, 108-115.
- 297 Li, H., Yan, S., Mao, H., Ji, J., Xu, M., Zhang, S., Wang, J., Liu, Y., & Sun, B. (2020).
298 Insights into maize starch degradation by sulfuric acid from molecular structure
299 changes. *Carbohydrate Polymers*, 229, 115542.
- 300 Liu, G., Gu, Z., Hong, Y., Cheng, L., & Li, C. (2017). Structure, functionality and
301 applications of debranched starch: A review. *Trends in Food Science & Technology*,
302 63, 70-79.
- 303 Liu, H., Xie, F., Yu, L., Chen, L., & Li, L. (2009). Thermal processing of starch-based
304 polymers. *Progress in Polymer Science*, 34(12), 1348-1368.
- 305 Liu, Z., Junejo, S. A., Zhang, B., Fu, X., & Huang, Q. (2022). Characteristics and
306 ethylene encapsulation properties of V-type linear dextrin with different degrees
307 of polymerisation. *Carbohydrate Polymers*, 277, 118814.

- 308 Qiu, C., Yang, J., Ge, S., Chang, R., Xiong, L., & Sun, Q. (2016). Preparation and
309 characterization of size-controlled starch nanoparticles based on short linear
310 chains from debranched waxy corn starch. *LWT - Food Science and Technology*,
311 *74*, 303-310.
- 312 Shi, J., Sweedman, M. C., & Shi, Y. (2018). Structural changes and digestibility of waxy
313 maize starch debranched by different levels of pullulanase. *Carbohydrate*
314 *Polymers*, *194*, 350-356.
- 315 Sun, B., Tian, Y., Chen, L., & Jin, Z. (2017). Linear dextrin as curcumin delivery system:
316 Effect of degree of polymerization on the functional stability of curcumin. *Food*
317 *Hydrocolloids*, *77*, 911-920.
- 318 Sun, Q., Gong, M., Li, Y., & Xiong, L. (2014). Effect of retrogradation time on
319 preparation and characterization of proso millet starch nanoparticles.
320 *Carbohydrate Polymers*, *111*, 133-138.
- 321 Vidal, N. P., Bai, W., Geng, M., & Martinez, M. M. (2022). Organocatalytic acetylation
322 of pea starch: Effect of alkanoyl and tartaryl groups on starch acetate performance.
323 *Carbohydrate Polymers*, *294*, 119780.
- 324 Wang, R., Li, Z., Zhang, T., Zhang, H., Zhou, X., Wang, T., Feng, W., & Yu, P. (2021).
325 Impact of amylose content on the starch branch chain elongation catalyzed by
326 amylosucrase from *Neisseria polysaccharea*. *Food Hydrocolloids*, *111*, 106395.
- 327 Zhan, W., Yuan, C., Cui, B., Yu, B., Liu, P., Wu, Z., & Zhao, H. (2021). Effect of chain
328 length on the structure and physicochemical properties of active compound/linear
329 dextrin composites. *Carbohydrate Polymers*, *269*, 118304.

- 330 Zhang, H., Wang, R., Chen, Z., & Zhong, Q. (2019). Enzymatically modified starch
331 with low digestibility produced from amylopectin by sequential amylosucrase and
332 pullulanase treatments. *Food Hydrocolloids*, 95, 195-202.
- 333 Zhang, H., Zhou, X., He, J., Wang, T., Luo, X., Wang, L., Wang, R., & Chen, Z. (2017).
334 Impact of amylosucrase modification on the structural and physicochemical
335 properties of native and acid-thinned waxy corn starch. *Food Chemistry*, 220, 413-
336 419.
- 337 Zhao, Y., Henry, R. J., & Gilbert, R. G. (2021). Starch structure-property relations in
338 Australian wild rices compared to domesticated rices. *Carbohydrate Polymers*,
339 271, 118412.

340 **Tables**341 **Table 1** Gelatinization parameters of starches

Sample	T_o (°C)	T_e (°C)
WMS	71.4 ± 0.1^c	88.08 ± 0.1^e
DWMS	58.8 ± 0.5^e	95.35 ± 0.2^c
S70	63.4 ± 0.6^d	91.08 ± 0.5^d
P70	87.9 ± 0.8^b	116.23 ± 0.1^a
S80	55.7 ± 0.1^f	85.57 ± 0.1^f
P80	94.0 ± 0.6^a	120.19 ± 0.0^b

342 Values are the means of three replicates \pm SD. Values with different letters in the same343 column are significantly different ($P < 0.05$).

344

Table 2 Molecular weight distribution of starches

Sample	< 1.6 k (g/mol) (%)	1.6k-5k (g/mol) (%)	5k-8k (g/mol) (%)	8k-80k (g/mol) (%)	80k-800k (g/mol) (%)	> 800k (g/mol) (%)
WMS	0.00 ± 0.00 ^e	0.00 ± 0.00 ^f	0.00 ± 0.00 ^f	0.00 ± 0.00 ^f	0.00 ± 0.00 ^e	100 ± 0.00 ^a
DWMS	23.67 ± 0.16 ^b	49.44 ± 0.06 ^c	11.88 ± 0.03 ^d	11.49 ± 0.06 ^c	1.53 ± 0.00 ^c	0.00 ± 0.00 ^b
S70	26.63 ± 0.19 ^a	56.82 ± 0.11 ^b	10.34 ± 0.08 ^c	6.20 ± 0.15 ^e	0.00 ± 0.00 ^d	0.00 ± 0.00 ^b
P70	9.87 ± 0.09 ^c	44.59 ± 0.04 ^d	18.13 ± 0.02 ^b	21.69 ± 0.01 ^a	2.81 ± 0.00 ^b	0.00 ± 0.00 ^b
S80	23.79 ± 0.18 ^b	57.20 ± 0.08 ^a	12.09 ± 0.04 ^c	6.92 ± 0.06 ^d	0.00 ± 0.00 ^d	0.00 ± 0.00 ^b
P80	9.47 ± 0.08 ^d	39.72 ± 0.04 ^e	26.64 ± 0.07 ^a	14.86 ± 0.07 ^b	5.07 ± 0.00 ^a	0.00 ± 0.00 ^b

345 Values are the means of two replicates ± SD. Values with different letters in the same

346 column are significantly different ($P < 0.05$).

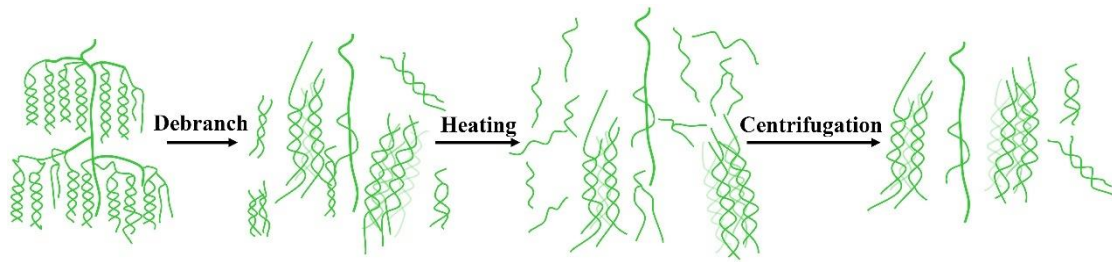
347 **Table 3** Chain length distribution of amylopectin of debranched starches

Sample	DP 6-12 (%)	DP 13-24 (%)	DP 25-36 (%)	DP \geq 37 (%)	Average DP (%)
DWMS	22.84 \pm 0.18 ^c	50.08 \pm 0.15 ^c	14.85 \pm 0.25 ^c	12.23 \pm 0.28 ^c	21.37 \pm 0.29 ^b
S70	25.68 \pm 0.21 ^a	52.77 \pm 0.24 ^a	13.63 \pm 0.16 ^d	7.92 \pm 0.26 ^e	19.47 \pm 0.22 ^d
P70	12.90 \pm 0.19 ^e	44.05 \pm 0.22 ^d	21.04 \pm 0.23 ^a	22.01 \pm 0.25 ^b	26.22 \pm 0.26 ^a
S80	24.00 \pm 0.22 ^b	50.93 \pm 0.28 ^b	14.72 \pm 0.17 ^c	10.35 \pm 0.29 ^d	20.58 \pm 0.30 ^c
P80	13.63 \pm 0.27 ^d	42.97 \pm 0.19 ^e	20.74 \pm 0.16 ^b	22.66 \pm 0.31 ^a	26.37 \pm 0.32 ^a

348 Values are the means of two replicates \pm SD. Values with different letters in the same

349 column are significantly different ($P < 0.05$).

350 **Figures**

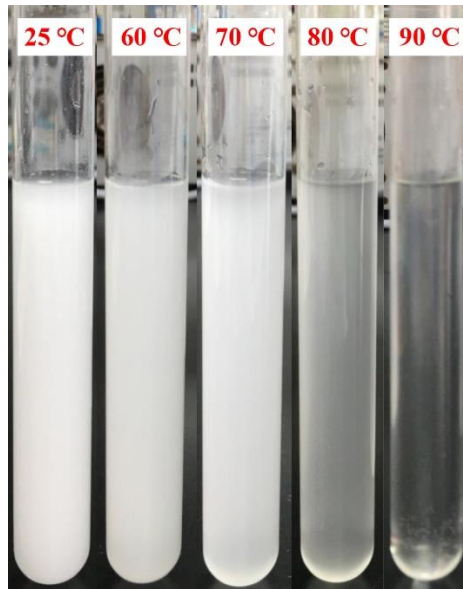


351

352

Figure 1 Schematic illustration of long linear dextrin fractions

Journal Pre-proof

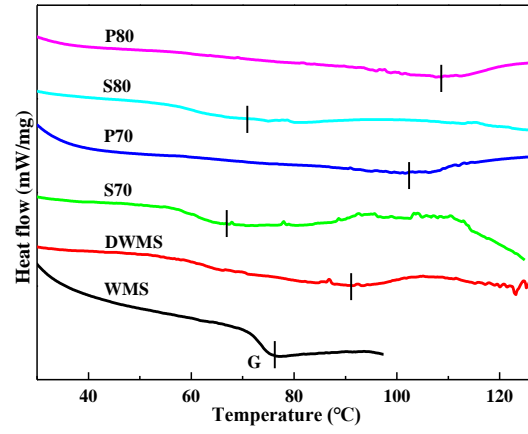


353

354 **Figure 2** Visual appearance of debranched starch solutions at different temperatures.

355

The concentration of debranched starch was 5% (w/v)

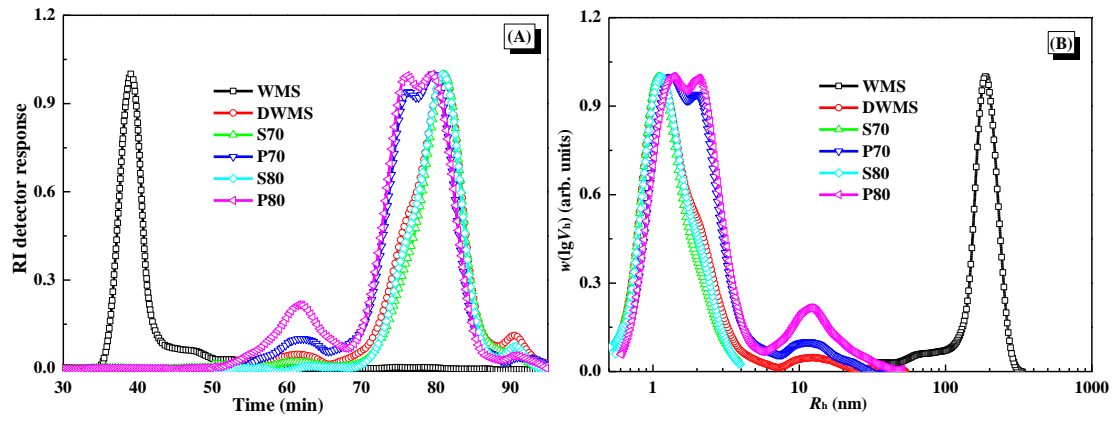


356

357

Figure 3 DSC curves of starches

Journal Pre-proof

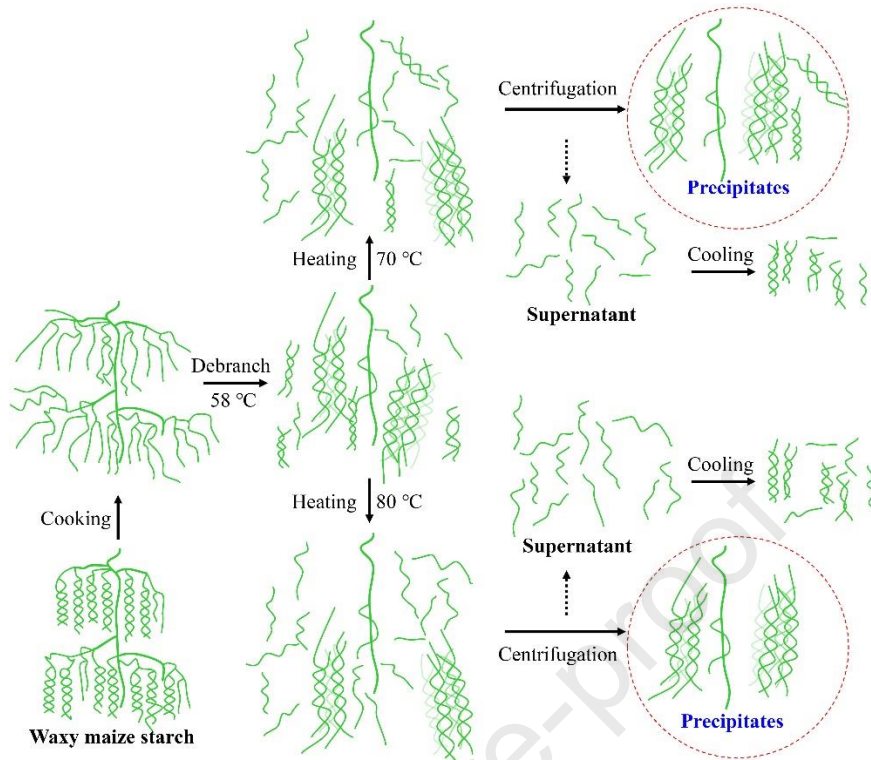


358

359 **Figure 4** RI response of SEC-RI chromatogram (A) and relationships between SEC

360

weight distributions ($w(\log(V_h))$) and molecular size (R_h) of starches



361

362 **Figure 5** Schematic illustration of starch structure changes during the fractionation of

363 long linear dextrans

- A method for isolating long linear dextrin from debranched starch was established.
- Ordered structure packed with long linear dextrin (LD) had high thermostability.
- Ordered structure was fractionated to obtain long LD by heating and centrifugation.
- Long LD content in starch was increased from 27.08% to 43.40% after the treatment.
- Short LD with polymerization units of 13-24 formed helical structure rapidly.

Conflict of Interest

The authors declare no competing financial interest.

Journal Pre-proof

Chengdeng Chi: conceptualization, literature analysis, investigation, writing, reviewing, and editing; Youcai Zhou: investigation and reviewing; Bilian Chen and Yongjin He: reviewing and editing; Yingting Zhao: writing, reviewing, and editing.

Journal Pre-proof